unambiguously between $J=\frac{1}{2}$ and $J=\frac{3}{2}$, unless the decay is isotropic. Isotropic decay also excludes $J=\frac{3}{2}$ if α is known from other evidence to differ from zero.

4. FINITE SAMPLES

When the measured $\langle P\rangle$ are subject to statistical errors, the asymmetry conditions exclude $J=\frac{3}{2}$ with large probability unless there is a satisfactory set α, I_μ which satisfies Eqs. (3.1) and (3.4) with reasonable probability. Although the $\langle P_L\rangle$ depend upon the momentum of the Ξ^-, it is possible to average all decay events in testing Eqs. (3.1), because the equations are linear in the $\langle P_L\rangle$ and α is fixed. Even production events from reaction (1.2) may be included, since the assumption of only two quantum states is not involved in Eqs. (3.1). In practice, a more severe test is obtained from a separate treatment of the Ξ^- produced in different cones about the axis of the K^- beam, so chosen that each $\langle P_L\rangle$ is nearly constant in each cone.

However, if the hypothesis $J=\frac{3}{2}$ "passes" the test (3.1), then the data must be divided into separate cones to perform the test (3.4). For typical possible values of α, one must solve Eqs. (3.1) for the I_μ and their correlated errors, using only data from reaction (1.1). Then if, for all values of α, the measured $|\langle P_{L2}\rangle|^2$ fail the test with high probability for some cone, or if they pass with only fair probability for each cone, $J=\frac{3}{2}$ is excluded with high probability.

PHYSICAL REVIEW VOLUME 129, NUMBER 4 15 FEBRUARY 1963

Nuclear Charge Distributions in the Interaction of 2.9-GeV Protons with Heavy Elements*

SHELDON KAUFMAN
Department of Chemistry, Brookhaven National Laboratory, Upton, New York
and
Department of Chemistry and Princeton-Pennsylvania Accelerator, Princeton University, Princeton, New Jersey
(Received 20 September 1962)

Cross sections for the formation of a number of nuclides in the mass range 65–74 in the bombardment of In, Au, and U with 2.9-GeV protons have been measured. Four isobars of mass 72, three of mass 67, and three of mass 66 are included. Charge distribution curves have been constructed from the data, using N/Z the ratio of neutrons to protons in the nucleus, as abscissa. The curves are not symmetric about the peak, falling less steeply toward large N/Z, with U having the most asymmetry. The peak position shifts to larger N/Z as the target mass increases. The data for In are consistent with a cascade-evaporation mechanism involving a long evaporation sequence, while the U data show the importance of low-excitation-energy fission in the formation of neutron-excess nuclides.

INTRODUCTION

RADIOCHEMICAL studies of the interaction of protons of energy in the GeV range with heavy elements (uranium,[1–4] lead,[3,5] and tantalum[6]) have led to the following general description of the mass-yield curve. The cross section for forming nuclides of a given mass number decreases as the mass number decreases, with no indication of any prominent fission peak, until low mass numbers are reached, where the cross section rises with decreasing mass number. There is a region of intermediate masses where the cross section is approximately constant. This behavior is in contrast to that observed at lower energies, where two distinct regions corresponding to spallation and fission are separated by a region of very low cross sections. It is evident from emulsion studies[7,8] that fission occurs to an appreciable extent at GeV energies, even with nuclei as light as Ag and Br. The problem is to determine the relation, if any, of the cross sections observed at these energies to the concepts of fission and spallation which have been useful at lower energies. A third process, fragmentation, which is a specifically high-excitation-energy process, has been postulated to account for the yields and excitation functions of nuclides with mass number less than about 40.

Previous work has shown that nuclides on both sides of the beta stability line are formed in appreciable amounts, and that stable nuclei, which are usually not

* Research performed under the auspices of the U. S. Atomic Energy Commission.
[1] R. H. Shudde, Atomic Energy Commission Document, University of California Radiation Laboratory Report UCRL-3419, 1956 (unpublished).
[2] C. L. Carnahan, Atomic Energy Commission Document, University of California Radiation Laboratory Report UCRL-8020, 1957 (unpublished).
[3] G. Friedlander and L. Yaffe, Phys. Rev. **117**, 578 (1960).
[4] B. D. Pate and A. M. Poskanzer, Phys. Rev. **123**, 647 (1961).
[5] R. L. Wolfgang, E. W. Baker, A. A. Caretto, J. B. Cumming, G. Friedlander, and J. Hudis, Phys. Rev. **103**, 394 (1956).
[6] J. R. Grover, Phys. Rev. **126**, 1540 (1962).
[7] N. A. Perfilov, O. V. Lozhkin, and V. P. Shamov, Uspekhi Fiz. Nauk **60**, 3 (1960) [Translation: Soviet Phys.—Uspekhi **3**, (60), 1 (1960)].
[8] E. W. Baker and S. Katcoff, Phys. Rev. **123**, 641 (1961); **126**, 729 (1962).

measured in radiochemical work, may represent much of the total yield of a given mass number. In order to determine the cross section for all products of the same mass number (the mass-yield), the charge distribution or isobaric yield curve must be determined to permit estimation of the cross sections of the unmeasured nuclides. Information about the mechanism of the reaction can also be obtained from this curve.[9]

Symmetric charge distributions have been observed in the fission of Th^{232} with 87-MeV protons[10] and U^{238} with 170-MeV protons,[11,12] by measurements of independent yields of nuclides over a small range in mass number. In a study of the fission of U^{238} with 340-MeV protons,[13] three isobars were measured for several mass numbers and a Gaussian curve was assumed. The charge distribution for the products of the fission of U^{238} and Bi^{209} with 480-MeV protons[14] was asymmetric, with the yields falling faster on the neutron-excess side. However, the latter result is based on nuclides of a wide range of mass numbers, and thus is less reliable than studies over a limited mass region. The yields for independent formation of Cs isotopes in the bombardment of U^{238} with 730-MeV protons have been determined,[15] indicating an asymmetric curve which falls more steeply toward the neutron-deficient side, in contradiction to the results of Lavrukhina and Krasavina. These data show that for uranium the width of the charge distribution increases with the bombarding energy, and the peak shifts toward less neutron-excessive nuclides.

The charge distribution for the mass range 38–48 observed[3] in the interaction of 3.0-GeV protons with Pb was poorly defined on the neutron-deficient side but there was an indication of a steeper fall than on the neutron-excess side, and the peak was close to the stability line. For the same nuclides formed from U^{238} at 3.0 GeV, the distribution was broader and the peak was one charge to the neutron-excess side of stability.

It thus seemed desirable to investigate further the isobaric yields from the interaction of GeV protons with heavy nuclei. The isobars of $A=72$ were chosen because there are four radioactive isobars with convenient half-lives and well-known decay schemes. Cross sections for these nuclides, three isobars of $A=66$, three isobars of $A=67$, and several other nuclides in the mass range 65–74 were measured, using indium, gold, and uranium targets.

[9] J. M. Miller and J. Hudis, Ann. Rev. Nucl. Sci. **9**, 159 (1959).
[10] B. D. Pate, J. S. Foster, and L. Yaffe, Can. J. Chem. **36**, 1691 (1958).
[11] P. Aagard, G. Andersson, J. O. Burgman, and A. C. Pappas, J. Inorg. Nucl. Chem. **5**, 105 (1957).
[12] A. C. Pappas and J. Alstad, J. Inorg. Nucl. Chem. **17**, 195 (1961).
[13] R. L. Folger, P. C. Stevenson, and G. T. Seaborg, Phys. Rev. **98**, 107 (1955).
[14] A. K. Lavrukhina and L. D. Krasavina, J. Nucl. Energy **5**, 236 (1957).
[15] Y. Y. Chu, Atomic Energy Commission Document, University of California Radiation Laboratory Report UCRL-8926, 1959 (unpublished).

TABLE I. Counting characteristics of nuclides studied.[a]

Nuclide	Half-life	γ-ray Energy (MeV)	Abundance
Ni^{65}	2.56 h	1.49	19.3%
Ni^{66}	55 h	1.04[b]	9 %
Cu^{67}	59 h	0.182	41 %
Ge^{66}	2.4 h	[c]	
Ge^{67}	19 min	[d]	

[a] Reference 17 contains data for other nuclides.
[b] Cu^{66} in equilibrium.
[c] Ga^{66} daughter counted.
[d] Ga^{67} daughter counted.

EXPERIMENTAL DETAILS

Bombardments were done in the circulating proton beam of the Cosmotron, at an energy of 2.9 GeV. The targets were metallic foils of the naturally occurring isotopes; thicknesses were 18, 50, and 48 mg/cm^2 for indium, gold and uranium, respectively. The foils were sandwiched between two 0.00025-in. aluminum foils to catch recoiling atoms, and 0.001-in. aluminum foils were used to monitor the proton beam. The cross section for the $Al^{27}(p,3pn)Na^{24}$ reaction used was 9.1 mb at 2.9 GeV.[16]

After the bombardment the target was dissolved with its recoil catchers and chemical separations performed, using the procedures outlined in the Appendix. The purified chemical fractions were counted with a calibrated 3×3-in. NaI crystal and a multichannel analyzer. The details of the counting and the γ-ray abundances used for most of the nuclides measured here have been published previously.[17] The half-lives and γ-ray abundances used for the remaining nuclides are given in Table I.[18] The aluminum monitor foils were counted with beta-proportional counters which had

TABLE II. Experimental cross sections, mb. Corrected independent cross sections are in parentheses. (I) denotes nuclides whose measured cross sections are independent.

Nuclide	Target In	Au	U
Ni^{65}	0.18 ±0.02	0.53 ±0.03 (0.48)	3.6 ±0.2 (3.1)
Ni^{66}	0.052 ±0.010	0.20 ±0.03 (0.18)	1.84 ±0.30(1.5)
Cu^{67}	0.29 ±0.03	0.71 ±0.07 (0.63)	4.7 ±0.2 (3.9)
Zn^{72}	0.0087±0.0009	0.072±0.009(0.066)	1.6 ±0.2 (1.3)
Ga^{66} (I)	3.5 ±0.2	0.49 ±0.05	0.49 ±0.06
Ga^{67} (I)	4.0 ±0.5	0.88 ±0.06	1.30 ±0.14
Ga^{72} (I)	0.23 ±0.02	0.57 ±0.04	4.2 ±0.3
Ga^{73}	0.087 ±0.009	0.21 ±0.03 (0.19)	2.7 ±0.2 (2.3)
Ge^{66}	0.16 ±0.02	0.015±0.004	0.004
Ge^{67}	0.68 ±0.12	0.075±0.009	0.033
As^{71}	6.2 ±0.8(5.7)	0.97 ±0.07 (0.90)	0.92 ±0.08
As^{72} (I)	7.3 ±0.8	1.80 ±0.13	2.4 ±0.1
As^{74} (I)	2.7 ±0.3	1.8 ±0.2	5.1 ±0.3
Se^{72}	2.8 ±0.5	0.37 ±0.05	0.19 ±0.03

[16] J. B. Cumming, J. Hudis, A. M. Poskanzer, and S. Kaufman, Phys. Rev. **128**, 2392 (1962).
[17] S. Kaufman, Phys. Rev. **126**, 1189 (1962).
[18] *Nuclear Data Sheets*, compiled by K. Way *et al.* (U. S. Government Printing Office, National Academy of Sciences–National Research Council, Washington, D. C.).

been calibrated for Na^{24} in Al by β–γ coincidence counting.

The Ge fraction was milked for Ga, and Ga^{66} and Ga^{67} were counted in order to determine their parents, Ge^{66} and Ge^{67}. Because of the low activity level of the milks, Ga^{66} was counted with a beta-proportional counter which was calibrated for that activity with sources of different thicknesses. Ga^{67} was counted with a 2-mm-thick NaI crystal and a single-channel analyzer, comparing it to a standard Ga^{67} source calibrated on the 3×3-in. crystal. There was too little Ni^{66} from the indium bombardments to detect in the presence of the large amount of Ni^{57} activity, so copper was milked and the Cu^{66} daughter counted.

The experimental cross sections are given in Table II. The error assigned to each cross section was obtained from the spread of individual determinations. Only one measurement was made of the cross sections of Ge^{66} and Ge^{67} from uranium; the uncertainty of these cross sections is estimated to be of the order of 30%. The systematic errors for most of the nuclides have been discussed before.[17] There is a 10% uncertainty in the Ni^{66} cross sections because of the uncertainty in the γ-ray abundance.[19]

The Ga^{66}, Ga^{67}, Ga^{72}, As^{72}, and As^{74} cross sections are

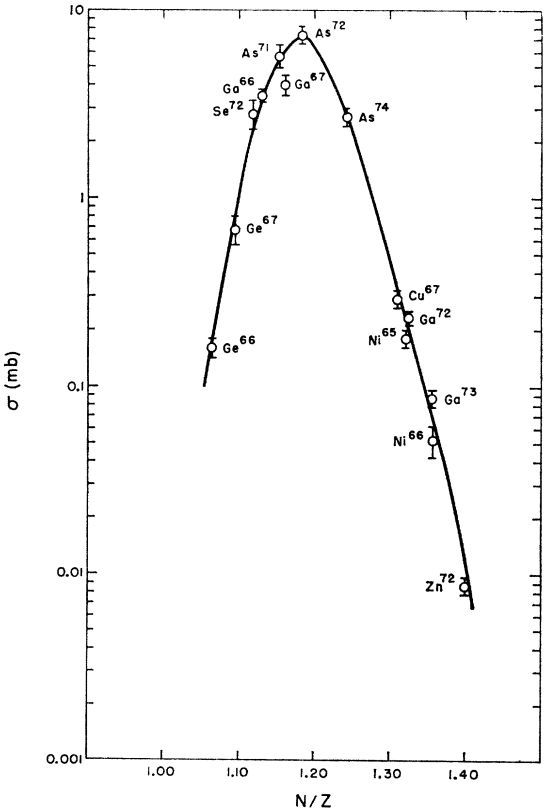

FIG. 1. Independent or corrected independent cross sections as a function of N/Z for indium plus 2.9-GeV protons.

[19] G. Friedlander and D. E. Alburger, Phys. Rev. 84, 231 (1951).

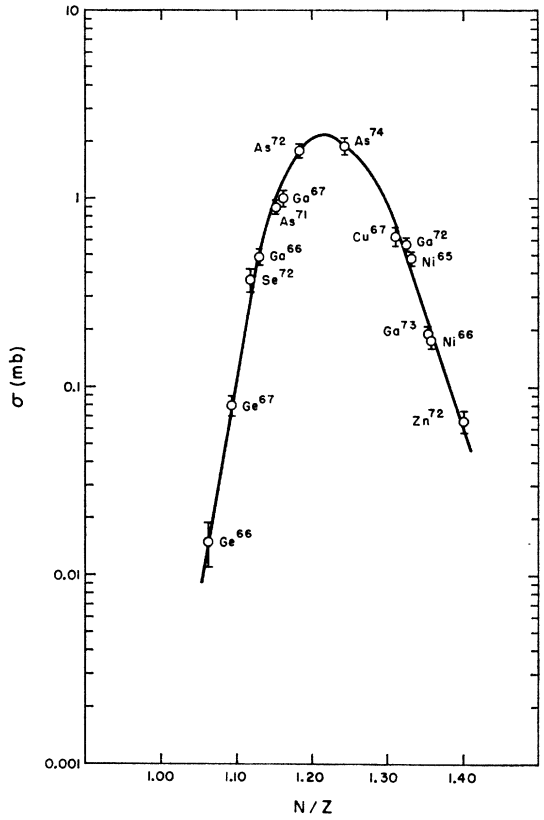

FIG. 2. Independent or corrected independent cross sections as a function of N/Z for gold plus 2.9-GeV protons.

for independent formation; the others are cumulative. In interpreting the data, independent cross sections must be estimated for the latter nuclides. This can be done with little uncertainty when the isobaric yield curve is steep, since the contribution from the decay of the precursors is negligible except for nuclides near the peak of the curve. However, one must first know enough independent yields to draw such a curve. It was necessary to use all of the cross sections, assuming that they all fall on the same curve, and to use a successive approximation technique to construct the isobaric yield curve.

In order to put different mass numbers on the same curve, one may choose as a reference the value of Z giving the largest binding energy for a given A, denoted by Z_A, and obtained from one of the semi-empirical mass formulas. Alternatively, one may use the ratio of neutrons to protons in the nucleus, N/Z. Both N/Z and $Z-Z_A$ were used to plot the data, and a smoother variation was found using N/Z as abscissa. The latter function was therefore used for convenience in interpolation.

The resulting curve for the indium cross sections showed that only As^{71} had an appreciable correction for the fraction formed by decay of the parent, about 10%. Corrections of a similar magnitude were made to several

TABLE III. Interpolated and total cross sections.

Target	In		Au		U	
Mass number	67	72	67	72	67	72
Interpolated cross section, mb	3.3±1.1	2.2±0.7	2.0±0.7	1.8±0.6	4.5±1.4	5.2±1.7
Total cross section, mb	8.3±1.2	12.5±1.2	3.8±0.7	4.6±0.6	10.5±1.4	13.6±1.7

of the cross sections in the gold bombardments. The corrections were larger for the neutron-excess nuclides in the uranium bombardments, and a somewhat arbitrary procedure was used, namely requiring that a smooth curve could be drawn through the corrected points, such that the experimental cumulative yields resulted upon summation.

The corrected independent cross sections are also given in Table II, in parentheses after the experimental cross section. Where no corrected value is given, the correction is smaller than 5%, and the cumulative yield is nearly independent. These independent and corrected cross sections are shown as a function of N/Z for each of the three target elements in Figs. 1–3. Smooth curves were drawn through the points without any attempt to fit specific functions, such as a Gaussian. Since one cannot assume any simple shape for the charge distribution curve, it is necessary to use as many points as are available in order to determine it. The curve shows the general trend, but it is not surprising that a few discrepant points are found, such as Ga^{67} for the indium curve. The uranium data were best fitted with separate curves for the neutron-excess nuclides of mass 65–67 and mass 72–73. While it is reasonable, as discussed below, that the yield decrease with mass number for the neutron-excess nuclides from uranium, the presence of two curves is not necessarily significant, since the curves plotted as a function of $Z-Z_A$ all have two branches on the neutron-deficient side, which are not apparent on the N/Z plots.

DISCUSSION

The isobaric yield curves in Figs. 1–3 all have a single peak, about which they are not symmetric, but fall off more rapidly to small N/Z. The peak is most neutron-deficient for indium, shifting to larger N/Z as the mass of the target increases. The slope of the neutron-deficient side of the curve remains almost constant, while the slope of the neutron-excess side decreases with increasing target mass. Thus the curve is widest for the heaviest target. The curve for arsenic targets[17] is symmetric on a N/Z plot, and is narrower than these curves.

The cross sections of unmeasured nuclides can be estimated from these curves, with an uncertainty of about 30% near the peaks. This was done for Zn^{67} and Ge^{72} in order to obtain the total isobaric cross section for these mass numbers, with the results given in Table III. The total cross section for $A=67$ is 20–30% lower than that for $A=72$ for all three targets. The uncertainty in the interpolated cross sections makes it difficult to be sure of the significance of this difference, while the similarity of the results for all three targets makes one suspect a systematic error, such as incorrect γ-ray abundances. The latter seems unlikely, however, because of the different proportions which a given nuclide contributes to the total cross section for the three different targets.

The total isobaric cross section in the region $38\leq A\leq 72$ from the interaction of lead with 3-GeV protons[3,5] has been estimated to be about 4 mb, in good agreement with the present results for gold. That found for the reactions of tantalum with 5.7 GeV protons[6] is 7.5 mb for $30\leq A\leq 100$.

The changes in yield of the various nuclides as a function of mass number of the target are shown most clearly if one plots the ratio of the cross section of a nuclide to the total isobaric cross section, or the fractional isobaric yield. This has been done, using the

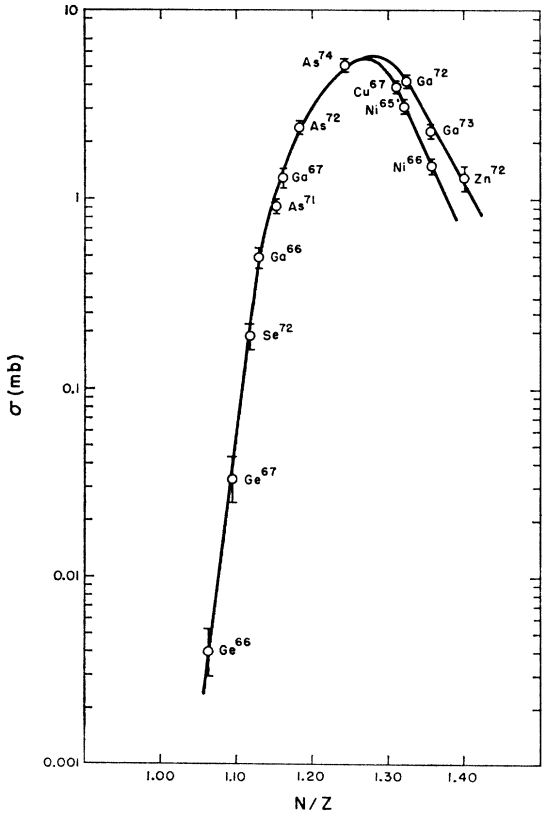

FIG. 3. Independent or corrected independent cross sections as a function of N/Z for uranium plus 2.9-GeV protons.

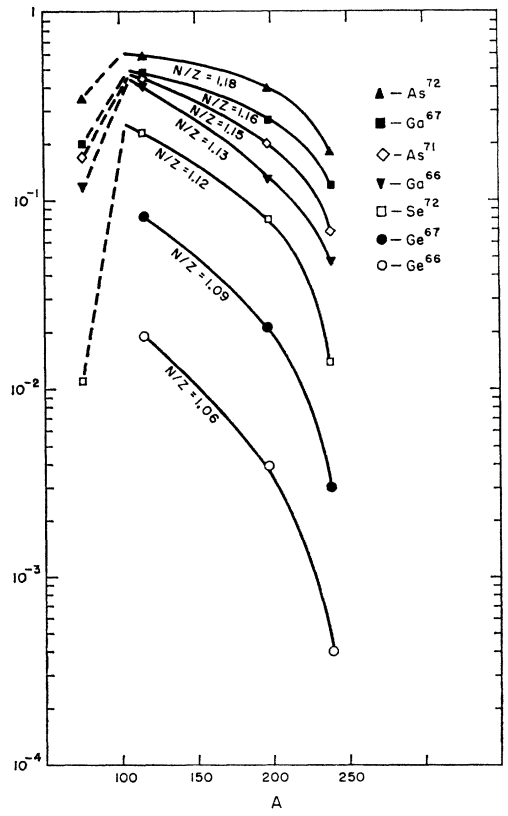

FIG. 4. Fractional isobaric yields as a function of target mass number, neutron-deficient nuclides.

corrected independent cross sections for each nuclide, and using the total cross section for $A=67$ for the nuclides of $A=65$–67 and that for $A=72$ for the nuclides of $A=71$–74. The neutron-deficient nuclides are shown in Fig. 4 and the neutron-excess nuclides in Fig. 5. The points for $A=75$ were obtained from previous work.[17]

As can also be seen from the charge distributions, the yields of neutron-deficient nuclides decrease with increasing mass of target above $A=115$, while the yields of neutron-excess nuclides increase. Moreover, the correlation with N/Z is excellent, as shown by Ga^{72} and Ni^{65}, both with $N/Z=1.32$, and Ga^{73} and Ni^{66}, with $N/Z=1.36$. The broken lines between the points at $A=75$ and $A=115$ are only to indicate the trend; they are not meant for interpolation. The yield of Se^{72}, for example, should increase rapidly above $A=75$, since the low yield there is probably due to the small cross section for the $(p,4n)$ reaction, rather than characteristic of the N/Z of the product. Except in the region between As^{75} and In^{115}, however, the smooth curves in Figs. 4 and 5 can be used for interpolation to other targets. With a value for the total isobaric cross section, this permits estimation of the cross section for any nuclide in the mass range $65\leq A\leq 74$ resulting from 3-GeV proton bombardment of any target heavier than In^{115}.

As pointed out in a recent review article,[9] a comparison of isobaric ratios found in low-energy compound nucleus reactions with results of high-energy studies enables one to judge the importance of evaporation processes. Table IV presents the isobaric ratios measured here which have also been measured in low energy alpha particle bombardments. The nuclide with the larger value of N/Z is in the numerator. The ratios observed in the indium bombardments are closest to the low-energy results, and indicate the importance of evaporation. The reason why the high-energy ratio is greater than the low-energy ratio for all the pairs is due to the wide distribution of evaporating nuclei in the

TABLE IV. Isobaric yield ratios from low-energy alpha-particle and 2.9-GeV proton reactions.

Nuclides measured	Alpha particle Target	Ratio	2.9-GeV protons In	Au	U	Reference
Cu^{67}/Ga^{67}	Cu^{65}	0.01[a]	0.071	0.73	3.6	c
Zn^{72}/Ga^{72}	Zn^{70}	0.014[a]	0.039	0.13	0.37	d
Ga^{66}/Ge^{66}	Zn^{64}	7.8[b]	23	32	127	e
Ga^{67}/Ge^{67}	Zn^{64}	2.5[b]	5.9	12	40	e
As^{72}/Se^{72}	Ge^{70}	1.7[b]	2.6	4.9	13	d

[a] Ratio at highest excitation energy; ratio is lower at lower excitation energies.
[b] Average ratio over most of range of excitation energy.
[c] N. T. Porile and D. L. Morrison, Phys. Rev. 116, 1193 (1959).
[d] S. Amiel, Phys. Rev. 116, 415 (1959).
[e] N. T. Porile, Phys. Rev. 115, 939 (1959).

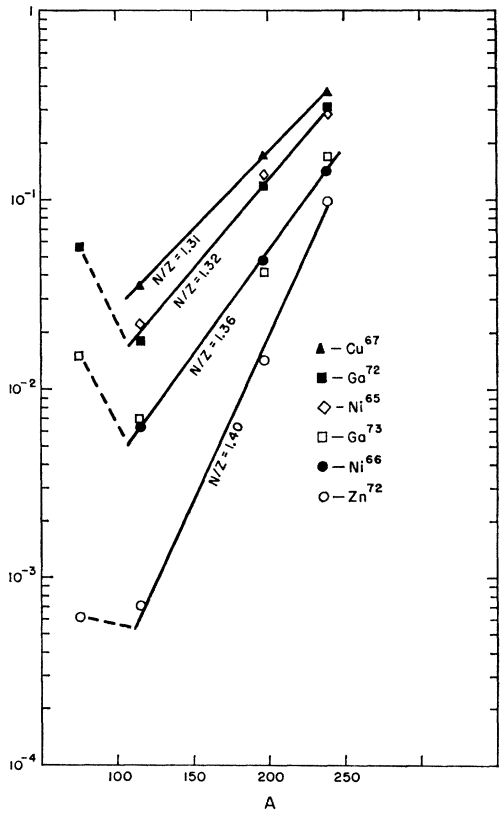

FIG. 5. Fractional isobaric yields as a function of target mass number, neutron-excess nuclides.

high-energy case, which makes it possible to form neutron-rich nuclides in greater yield. The very large ratios observed for gold and uranium show that if evaporation plays a part, the average precursor nucleus is more neutron excess than the compound nucleus formed in the alpha-particle bombardments.

The charge distribution curves can be understood in terms of two alternative paths for the formation of these nuclides: a high excitation energy-evaporation path and a low excitation energy-fission path. In reality, there is a continuous gradation of processes, but it is convenient to idealize them into these two extremes. The evaporation process produces the final nuclei as a result of a large number of evaporation steps, starting from a highly excited nucleus. The latter may be left after the fast cascade is over, or it may even be the result of a fission or fragmentation. The essential characteristic is that an appreciable number of units of charge and mass be lost in the evaporation. The fission-low excitation energy process refers to events in which the fragment has relatively little excitation energy, and therefore is close to the mass of the final product, since relatively few nucleons can be evaporated. Also included in this group are fission events occurring at the end of an evaporation sequence, provided the fission fragments are not appreciably excited.

The most probable value of N/Z along the evaporation chain can be estimated by combining the results of the fast cascade calculations[20] with those of the evaporation calculations.[21] Comparison with the experimental values for each target will indicate the importance of the evaporation mechanism. Extrapolation of the results of reference 20 to 2.9 GeV indicates the following as the most probable cascade products and excitation energies: Rh^{105} excited to 350 MeV from In^{115}; Os^{186} excited to 500 MeV from Au^{197}, Ac^{227} excited to 500 MeV from U^{238}. The distribution of excitation energies about the most probable value is quite broad, and thus a wide range of evaporation products may be formed from a few cascade products. The distribution in Z and A of the cascade products is also rather broad, so the above nuclides and energies are only representative examples.

Taking first the case of In^{115}, the results of reference 21 indicate that a highly excited nucleus close to the stability line will become more neutron-deficient; e.g., if Rh^{105} loses 33 mass numbers, the most probable number of charges lost will be 12, and the most probable isobar of mass 72 will be As^{72}, in agreement with the experimental charge distribution. The same result is obtained for any nuclide in this mass region close to the stability line which is given just enough excitation energy to result in a mass 72 product. Moreover, the effect of changing the position of the initial nuclide with respect to stability by as much as 3 units of charge is to alter the relative proportion of charged particles evaporated so as to lead again to As^{72} as the most probable product. Thus the charge distribution observed in this mass region from the interaction of 2.9-GeV protons with indium is satisfactorily accounted for by a cascade-evaporation sequence.

The amount of excitation energy required to produce nuclides of mass 72 from gold by a cascade-evaporation process is so large as to make this a highly improbable one. The most likely mechanism seems to be a fission during the evaporation stage which produces an excited fragment heavier than mass 72 which then loses mass by further evaporation to lead to the observed products. A fragmentation process in which the complementary fragment to the light one was highly excited is another possibility.

Comparing the gold curve to the indium curve, the larger N/Z at the peak for gold implies a much shorter average evaporation chain, which would not completely wash out the effect of the initially neutron-excess excited fragment. The latter is assumed to have a value of N/Z less than 1.45, corresponding to the average cascade product from gold, and assuming the constant-charge-ratio hypothesis[22] of high energy fission. The smaller slope of the neutron-excess side of the charge distribution curve also indicates a shorter evaporation path for gold than for indium. No information about the point along the evaporation path at which fission occurs can be obtained from these data, because the peak of the charge distribution is independent of the proportion of evaporation occurring before fission.

The difference between uranium and gold is partly due to the large probability of low excitation energy fission of the former. The specifically high energy processes would be expected to shift the charge distribution curve to higher N/Z for uranium, but this effect is enhanced by the formation of typically neutron-excess fission products as a result of relatively low excitation energy fission. The small slope of the neutron-excess wing of the curve is probably the result of this effect, and the lower cross sections for masses 65–67 may be due to the steep fall of the mass-yield curve for low energy fission[23] in this region. The large contribution of low excitation energy fission arises from the relatively large probability of small energy transfers from GeV protons,[4] and the fissionability of nuclides in the region of uranium.

In summary, it appears that the fissionability of uranium has still a major influence on its nuclear reactions, even at GeV energies. Although neutron-deficient nuclides are formed which are not formed at lower energies, their cross sections decrease rapidly away from the stability line, and the neutron-excess nuclides constitute the major portion of the mass-yield in this mass region. With lighter targets, evaporation

[20] N. Metropolis, R. Bivins, M. Storm, J. M. Miller, G. Friedlander, and A. Turkevich, Phys. Rev. **110**, 204 (1958).
[21] I. Dostrovsky, P. Rabinowitz, and R. Bivins, Phys. Rev. **111**, 1659 (1958).
[22] R. H. Goeckerman and I. Perlman, Phys. Rev. **76**, 628 (1949).
[23] P. C. Stevenson, H. G. Hicks, W. E. Nervik, and D. R. Nethaway, Phys. Rev. **111**, 886 (1958).

plays a major role, and the maximum yields are found on the neutron-deficient side. It would be of interest to extend the charge distribution curves by measuring short-lived precursors to see if there is a continued decrease of yield on either side of the peak. Mass-spectrometric measurements of the stable nuclei would, of course, be very helpful in determining the shape of the curve.

ACKNOWLEDGMENTS

The author is grateful to Dr. R. W. Dodson and Dr. G. Friedlander for making it possible for him to use the facilities of Brookhaven National Laboratory during the course of this research, and to the Chemistry Department of Princeton University for the grant of a leave of absence. Discussions with colleagues at both Brookhaven and Princeton were helpful. Special thanks are due the members of the Analytical group at Brookhaven, under Dr. R. W. Stoenner and Dr. J. K. Rowley, for ably performing the chemical yield determinations.

APPENDIX. CHEMICAL PROCEDURES

Indium and uranium foils were dissolved in conc. $HCl+H_2O_2$, and gold in $HCl+HNO_3$. When Ge was to be separated, $GeCl_4$ was immediately distilled in a stream of chlorine. Next As and Se were distilled as halides in a stream of HBr. The further purification steps are described under the individual elements.

Nickel. An acid sulfide scavenge was done, after which the H_2S was boiled out and excess NH_4OH added, precipitating In or U, if they were the target. The filtrate was further scavenged with $Fe(OH)_3$, and Ni dimethylglyoxime precipitated. It was dissolved in HCl, two Pd dimethylglyoxime scavenges done, then two acid sulfide scavenges. Finally Ni dimethylglyoxime was precipitated in the presence of citrate. In the case of In bombardments, a portion was used to milk Cu^{66}, about 30 min after the final purification.

Copper. The acid sulfide precipitate (also containing Au if that was the target) was dissolved in $HCl+HNO_3$, boiled to expel the HNO_3, and saturated with SO_2 to precipitate Au (carrier was added in the In and U bombardments). CuSCN was precipitated from the solution, the precipitate dissolved, and two AgCl scavenges done. NaOH in excess was added, KCN was added, and CdS and As_2S_3 were precipitated. The filtrate was acidified and the HCN boiled out, precipitating CuS. This was dissolved and a final CuSCN precipitation done.

Zinc. The solution remaining after the Ga extraction was boiled to dryness, taken up in 0.5*M* HCl, and passed through a Dowex-1 anion exchange column. After thorough washing with 0.5*M* HCl, Zn was eluted with 0.01*M* HCl, leaving any Cd still on the column. The eluate was made 6*M* in HCl and extracted with ethyl ether. Ga carrier was added and milked after 1–2 days.

Gallium. The HBr solution after the As and Se distillation was made 7*M* in HBr and extracted with β, β'-dichlorodiethyl ether. The ether was washed with 9*M* HCl to remove In and then with 1*M* HCl to remove Ga. The Ga was scavenged with acid sulfide precipitations and $Fe(OH)_3$ precipitations. A final extraction from 6*M* HCl into diethyl ether was done, and Ga precipitated as the oxine.

Germanium. The Ge distillate was saturated with H_2S and the GeS_2 dissolved in NaOH. A second distillation of $GeCl_4$ was done, Ga carrier added to the distillate, and Ga milked after 4–8 h. The Ga milk was purified by acid sulfide scavenges and diethyl ether extraction.

Arsenic and *Selenium.* These elements were purified as described previously.[17]